Background and Progress Report

For individual project

Jonas Brami

1 June, 2022

Contents

1. Introduction

The problem we aim to solve during this project is the placement of a sensor on a specific target point on a surface using a fixed manipulator arm mounted on the top of an unmanned quadcopter. A quacopter is an underactuacted helicopter with four rotors. This UAV (Unmanned Aerial Vehicles) is underactuated because arbitrary configurations and trajectory cannot be realized.
In the last ten years, research about UAV controls accelerated drastically with many applications in the civilian industry in a variety of areas.
Monitoring and sensing tasks are traditionally operated by human but can be complicated (require expert, highly trained technicians), expensive, and dangerous for the human operator (when the point of interest is hard to reach, the human manipulator may need special training and equipement to reach the point of interest). For example, big structures like bridges need to undergo regular inspections to ensure there are no cracks or other signs of structural fatigue.
Using UAVs for such tasks would not only reduce cost of maintance of those structures, but also increase the security of both the human manipulator and the civilians using it.
Sensor placement on surfaces using UAVs is an active field of research and we will propose a solution based on velocity fields.

A velocity field is a function taking as input a four dimensional vector (x, y, z, t) and returning a 3 dimensional velocity vector (u, v, w).
Since our environment is static, meaning that the obstacles and goal are not moving, we will always use a time invariant velocity field. Diverse ways of placing sensors using UAVs have been explored in the past, including but not limited to:

- Direct Placement: Using a fixed arm manipulator on an UAV, we use the force exerted by the thrust of the UAV to provide enough pressure on the tip of the arm to place the sensor on the target point.
- Sensor Launching [1]: Using the energy stored in a spring, the UAV ejects the sensor at the desired velocity to reach and attach to the target (Unmanned Aerial Sensor Placement for Cluttered Environments). This strategy is very useful when it is not physically possible for a mounted arm to reach the target however it suffers from small payload capacity.
- Drop from flight: We simply drop the sensor above the target point. When target accuracy is not a priority and we are aiming at a non-vertical surface and there is no occlusion above the target, this sensor placement strategy is the most effective.

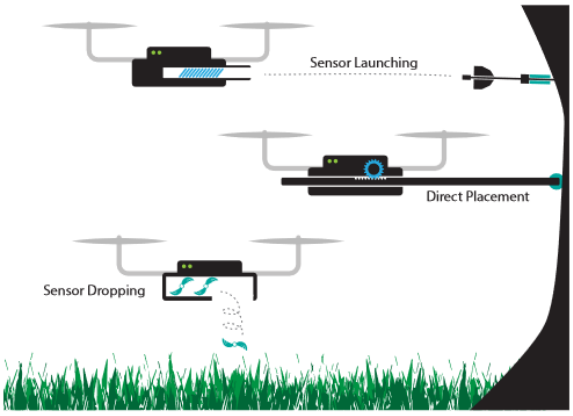

	Direct [7]	**Drop** [2]	**Launch** [i]
Accuracy	±0.025 m	±4 m	±0.1 m
Safety distance	0 m	>10 m	4 m
Payload	1.85 kg	10 kg [ii]	0.65 kg
Sensor number	single	multiple	expandable

Figure 1: Different types of sensor placement from [1]

The characteristics of each one of mentioned methods are shown in 1. We decided to go through with the Direct Placement strategy because despite its simplicity, it provides good accuracy and is able to place a large variety of payloads. The solution we will propose can be divided in 3 parts: The first is environment mapping where we perform surface and obstacle recognition using live depth sensor feed. The second part is designing a potential based velocity field to perform path-planning by guiding the UAV from the start point to the target point. The third and last part is designing a velocity field around the target point to apply the desired force amplitude. In this part, we will use the passive velocity field controller (PVFC) to optimize our energy consumption.

2. Literature Review and Theory

2.1. Current State of the art for UAM

There exists 2 main approaches for controls of unmanned aerial manipulators: The first one is the centralized approach where we consider the manipulator and the UAV as a whole whereas the decentralized apporach the manipulator control and UAV control are independant problems. In the case of the Sensor placement with a quadcopter, we use the centralized approach because the arm has no degree of freedom and the force exerted by the

tip is coming from the thrust of the UAV. The centralized approach is often built on top of a model-based full state control loop optimized with LQR (Linear–quadratic regulator) around some desired state. In [4], the author present the current state of the research for UAMs. An UAM can be divided into 4 elements: The UAV floating base (in our case, a quadcopter), the robotic arm, a sensor/gripper attached to the end of the arm (in our case, a sensor will be attached to the end of the arm), diverse sensors on UAV to handle perception (the depth camera)

2.2. Velocity field path-planning for single and multiple unmanned aerial vehicles

In [1], the author presents a path-planning technique based on velocity fields generated from potentials solution of Laplace's equation. Two different types of solution to potential V for the Laplace

$$\nabla^2 V = 0$$
$$\frac{\partial^2 V}{\partial x^2} + \frac{\partial^2 V}{\partial y^2} = 0 \tag{1}$$

equation are presented in this paper: Type 1 are irrotational solutions to generate sink and source fields and Type 2 solutions are used to build solenoidal fields.

$$V_1 = Q_1 \ln\Big((x_1 - \tilde{x_1})^2 + (x_2 - \tilde{x_2})^2\Big) \tag{2}$$

$$V_2 = Q_2 \arctan\left(\frac{(x_2 - \tilde{x_2})}{(x_1 - \tilde{x_1})}\right) \tag{3}$$

where (x_1, x_2) is the position of the UAV, $(\tilde{x_1}, \tilde{x_2})$ is the position of the obstacle; V_1 and V_2 are respectively type 1 solution (source field) and type 2 solution (vortex field).
The author justifies the use of Laplace solution for building the velocity field for multiple reasons:

- The use of Laplace solution for potential guarantees the uniqueness of the minimum in the field. Specifically, the use of vortex function built from shaping function to circle around obstacle will ensure that only the goal point will be a minimum of the field and that the UAV will not get stuck at some local minimum. As the author states, we can do an analogy with a famous strategy to find the exit of a maze: by keeping a hand on a wall of the maze and walking while always touching the wall, we are ensured to find the end of the maze. This is far from being an optimal solution, however, it can guarantee that the goal will be reached. As a result, those solenoidal fields based on vortex function also provide active collision avoidance.
- Scalar shaping functions are at the base of these methodology because by crafting them to match the shape of the obstacles, we are able to generate corresponding vortex functions for obstacles of any shape. Since the vortex field is defined for each obstacle, it would be easy to reevaluate the field after addition or removal of an obstacle.
- Finally, irrotational solutions of the Laplace equation allow us to enforce an exclusion radius around obstacles (source field) and to direct the UAV in direction of the target point (sink field). The exclusion radius is encoded using the amplitude Q_1 of the irrotational field.

We can leverage these both types of potentials to derive a velocity field that will guide the UAV to the contact point without colliding with the surface. For example, we could define the exclusion radius to be the distance between the centre of mass (CoM) of the quadcopter and its most distant part on the quadcopter. We will still be able to make contact because the distance between the tip of the arm and the CoM will be longer than this exclusion radius.

2.3. Spherical field to maintain desired force

When contact has been made, we suppose that the surface static friction coefficient is high enough to maintain the contact. Since the arm has a fixed size and does not move, this section will describe a velocity field on the surface of a sphere around the target point with a radius defined by the distance between the CoM of the quadcopter and the tip of the arm.
Computing the field on the surface of a sphere is very computationally efficient because we do not have to sample field vectors in the whole 3d space around the point of interest. First we need to compute the feasible position of the CoM to apply the desired force. We know that this position is unique because there is only one vertically stable pitch for a given desired force amplitude. The quadcopter needs to pitch to have a forward velocity because the quadcopter is underactuacted.
We can either compute this position analytically or we can use machine learning techniques such as regression to compute the feasible pitch as a function of the desired force. The latter option would require collecting training data from simulations on Gazebo. Now we can generate the velocity field on the surface of the sphere to point on the tangent direction of the sphere in the direction of the stable pitch position.
This field will have an amplitude proportional to

the distance from this point. The planning strategy we described would also allow us to easily define a desirable range for the yaw angle depending on the type of sensor and on the friction coefficient of the target surface. Finally, we use a Passive Velocity Field Controller [2] to follow this field to minimize the loss of kinetic energy to the environment when interacting with the surface. Now we are going to describe how the spherical field is computed. Let us recall that the cartesian to spherical change of variable is defined as

$$r = \sqrt{(x^2 + y^2 + z^2)}$$

$$\theta = \arccos\left(\frac{z}{r}\right)$$

$$\phi = \begin{cases} \arctan\left(\frac{y}{x}\right), & \text{if } x > 0, \\ \arctan\left(\frac{y}{x}\right) + \pi, & \text{if } x < 0 \text{ and } y \geq 0, \\ \arctan\left(\frac{y}{x}\right) - \pi, & \text{if } x < 0 \text{ and } y < 0, \\ \pi/2, & \text{if } x = 0 \text{ and } y > 0, \\ -\pi/2, & \text{if } x = 0 \text{ and } y < 0, \\ notdefined, & \text{if } x = 0 \text{ and } y = 0 \end{cases} \tag{4}$$

The jacobian defining the curvature of the sphere for at each point for this transformation is

$$J = \frac{\partial(x, y, z)}{\partial(r, \phi, \theta)}$$

$$J = \begin{bmatrix} \sin(\theta)\cos(\phi) & \cos(\theta)\cos(\phi) & -\sin(\phi) \\ \sin(\theta)\sin(\phi) & \cos(\theta)\sin(\phi) & \cos(\phi) \\ \cos(\theta) & -\sin(\theta) & 0 \end{bmatrix} \tag{5}$$

We can now derive this velocity field in 3 steps:

1. Sample a list of point on the surface of the sphere in cartesian coordiate. In Python or Matlab, a meshgrid can be used where we the field will be non zero with
$$x^2 + y^2 + z^2 - R_{sphere} \leq \epsilon$$
2. For each point in the list, we compute its spherical coordinate according to 4 and we compute the jacobian at the point
3. Let $(\phi_{opt}, \theta_{opt})$ be the desired position on the sphere. For each point $/vec(\phi, \theta)$ on the sphere , we compute the tangeant vector in the the field that will point toward the goal as $J(r, \phi, \theta).(\epsilon, \phi_{opt} - \phi, \theta_{opt} - \theta)^T$ using the jacobian defined in 5

2.4. Passive Velocity Field Control of Mechanical Manipulators

In [2], the author explains the advantages of encoding a contour following task using velocity fields. He later presents the passive velocity field controller whose objective is to "maintain an energetically passive relation-ship between the manipulator under closed loop control and its physical environment, while causing the manipulator to perform the desired task." We will explain each one of those arguments and relate them to our sensor placement task.

2.4.1. Velocity fields for planning

The classical approach to do planning is to encode the task into a timed trajectory $Q : \mathbb{R}_{\geq 0} \rightarrow G$ where G is the n-dimensional configuration manifold for the manipulator. Using this strategy, the objective of the controller is to minimize the deviation between $q(t)$ and $Q(t)$ where $q : \mathbb{R}_{\geq 0} \rightarrow G$ is the actual coordinate representation of the manipulator. This strategy could be fine if the manipulator was able to never deviate from the timed trajectory defined by Q. However, this is rarely the case and when a deviation occurs, a side effect of this minimization strategy called radial reduction can occur. The author argues that if following the

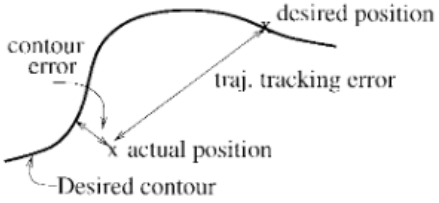

Figure 2: radial reduction from [2]

path of the desired trajectory is more important than the timing in which the manipulator follows this trajectory, a strategy based on velocity field is more appropriate because the velocity of the manipulator will only depend on its current position and will be time invariant. For the sensor placement task, using a timed trajectory strategy with deviation minimization to reach the contact point may lead the UAV to collide with an obstacle. With our strategy based on potential velocity field, the UAV will not try to shortcut the desired path in case of deviation.

2.4.2. Passive velocity field controller

The controller presented in this paper allows storing kinetic energy of the manipulator's actuators in a spring or a flywheel and releasing it when needed so that we can interact with surfaces while minimizing energy loss. This is useful because the UAV has a limited amount of energy stored in its battery and this is one of the main limiting factors for most tasks (including Sensor Placement).
To present this concept, the author first define the

notion of a passive dynamic system:
A dynamic system with input $u \in U$ and output $y \in Y$ is passive with respect to the supply rate $s : U \times Y \to \mathbb{R}$, if for any $u : \mathbb{R}_{\geq 0} \to U$ and for any $t \geq 0$ the following relation is satisfied:

$$\exists\, c \in \mathbb{R}$$
$$\int_0^t s(u(\tau), y(\tau))d\tau \geq -c^2 \tag{6}$$

This supply rate can be seen as the total mechanical power input: $s(\tau_{tot}^T \dot{q})$. Here the input τ_{tot} is the total force exerted on the manipulator and $\dot{q}$ is the velocity of the manipulator. When considering a feedback system interacting with the environement shown in figure 3, we can decompose $\tau_{tot} = \tau_e + \tau$ (where τ and τ_e are respectively the forces generated by the actuators and the external forces, for example the contact force when touching a surface), we can derive the power generated by external forces as $s(\tau_e \dot{q}) = \tau_e^T \dot{q}$. As explained in the

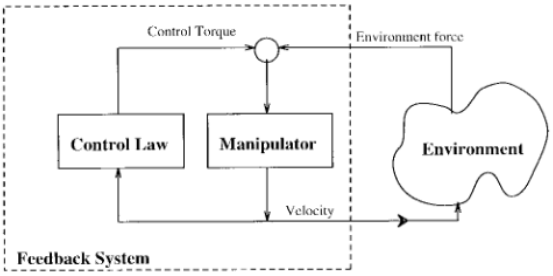

Figure 3: PVFC loop [2]

paper, a system defined by this supply rate is not passive because obstacles may bring the manipulator to a complete stop for an unbounded amount of time and this loss of kinetic enery cannot be bounded. As a result, the passivity relation

$$\int_0^t \tau_e^T \dot{q} d\tau \geq -c^2 \tag{7}$$

is not valid here because the l.h.s represents the total amount of energy lost to the environment and, as stated before, it cannot be bounded. This issue motivates the introduction of an augmented system: a fictitious flywheel is added to the system that acts as an energy storage element. The dimensionality of the manifold is then increased by one to include the state of the flywheel and this augmented state will be noted as

$$\bar{q} = [q_1, ..., q_n, q_{n+1}] \tag{8}$$

The paper later presents the dynamics of this augmented state and designs a field for the fictitious flywheel such that "the kinetic energy of the augmented system remains constant"

3. Technical Experimentation

In this section, we will present the field we previously described with illustrations. The field in

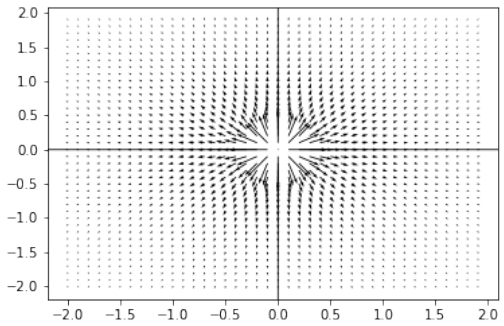

Figure 4: Simple Type 1 irrotational source

figure 4 was drawn by computing the gradient of V_1 with $(\tilde{x_1}, \tilde{x_2}) = (0, 0)$.

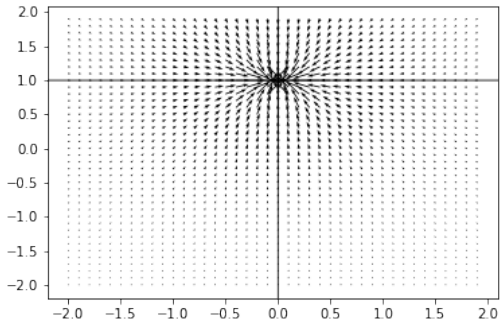

Figure 5: Simple Type 1 irrotational sink

The field in figure 5 is a sink field at $(0, 1)$, it is similar to the source field in figure 4 but with opposite sign.

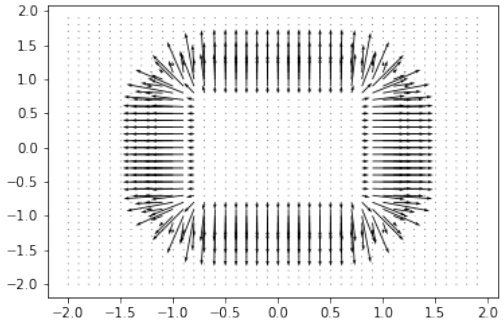

Figure 6: irrotational field from shaping

The field in figure 6 has been generated by computing the gradient of the shaping function of a superquadratic:

$$H = (x_1 - \tilde{x_1})^n + (x_2 - \tilde{x_2})^n \tag{9}$$

$$F = \frac{1}{1 + (\frac{1}{L} H^{\frac{1}{n}})^m} \tag{10}$$

As stated in [3], when $m \gg 1$, the edge of the shaping function gets thinner. Higher values of n result in more rectangular shapes whereas $n = 2$ describes the shaping function of a sphere.

Both these fields are type 1 irrotational solutions of the Laplace equation.

By adding the irrotational sink from figure 5 and the irrotational field from shaping function in figure 6 we obtain a good representation in figure 7 of what the velocity field will look like when close to the target point.

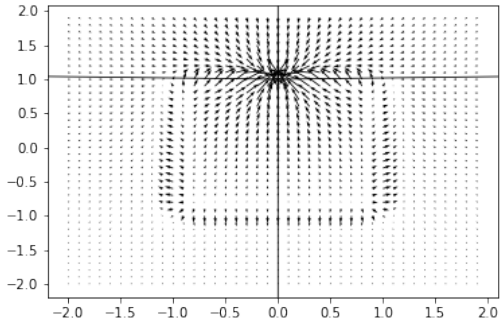

Figure 7: irrotational field from shaping with sink

The shaping function is mainly used to generate a vortex field around an obstacle, as explained in the paper. It is given by:

$$v_2 = -\frac{\partial F}{\partial x_2} e_1 + \frac{\partial F}{\partial x_1} e_2 \tag{11}$$

Here, e_1 and e_2 are an orthonormal basis.
We can see in figure 8 an example of vortex field around a super quadriatic.

As explained in section 2, after we made contact, we stop using the potential based field and we use the spherical field to maintain contact with the desired force. Figure 9 represents an example of such a field where the red point is the optimal position to apply the pressure, the blue arrows are the velocity field vectors and the center of the sphere is the point where the pressure is applied

4. Project Plan

- Implement the potential based planning and spherical velocity field in a simple simulation with the quadcopter dynamics (Expected to be done by Jun 2nd)

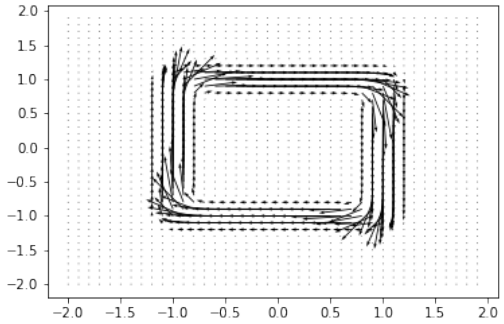

Figure 8: Solenoidale field from shaping function

- Implement and integrate these velocity fields into the ROS (Robot Operating System) passive velocity field controller written by Brett Stephens. ROS is a set of open source programs which main functionnality is to provide a subscription base communication system between ROS Nodes and many useful abstractions for robotics. (Expected to be done by end of June)

- Use the Depth Camera D435i to generate the field with the live sensor data using the Point Cloud Library [5] (PCL). PCL is a software providing large scale point cloud processing capabilities. (Expected to be done before mid July)

- Train a machine learning model to compute the optimal pitch vector taking as input the profile of the quadcopter (moments of inertia, mass...), surface normal at the point of interet, and the desired applied force on the target point. (Expected to be done by end of July)

  A measure of success for this project could be to succesfully implement the whole pipepile from perception to velocity fields together with PVFC and making it work with a real quadcopter in the lab. A first success would be to have it working without obtacles and with a simple vertical target surface. When we have this working, a full success would be to have it working for diverse kind of obstacles and non trivial target surfaces. A total success would be to be able to maintain contact with the target when applying external forces/torques on the UAV.

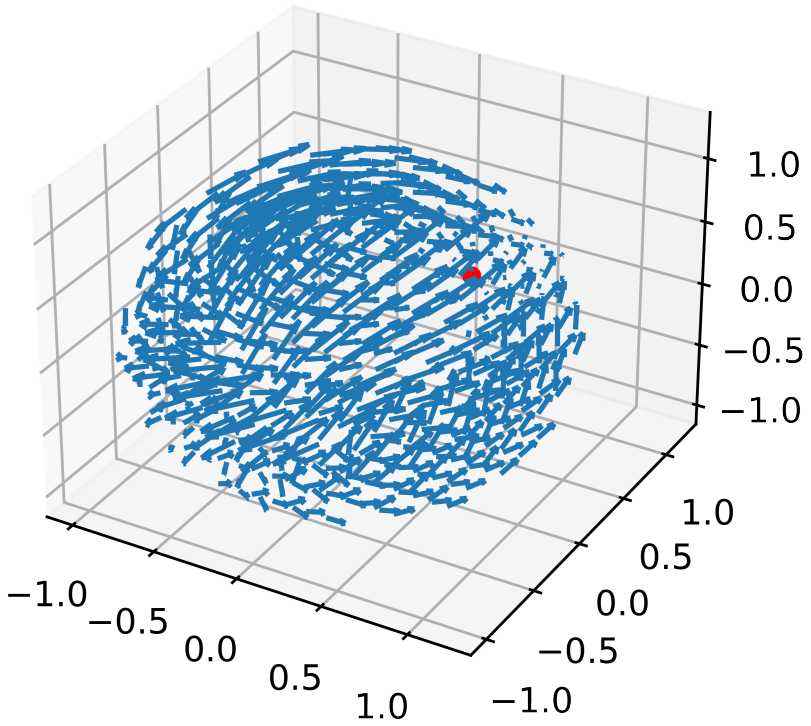

Figure 9: Spherical contact field

References

[1]A. Farinha, R. Zufferey, P. Zheng, S. F. Armanini, and M. Kovac, ≪Unmanned aerial sensor placement for cluttered environments≫, IEEE Robotics and Automation Letters **5**, 6623–6630 (2020).

[2]P. Y. Li and R. Horowitz, ≪Passive velocity field control of mechanical manipulators≫, IEEE Transactions on robotics and automation **15**, 751–763 (1999).

[3]C. McInnes, ≪Velocity field path-planning for single and multiple unmanned aerial vehicles≫, The Aeronautical Journal **107**, 419–426 (2003).

[4]F. Ruggiero, V. Lippiello, and A. Ollero, ≪Aerial manipulation: a literature review≫, IEEE Robotics and Automation Letters **3**, 1957–1964 (2018).

[5]R. B. Rusu and S. Cousins, ≪3d is here: point cloud library (pcl)≫, in 2011 ieee international conference on robotics and automation (IEEE, 2011), pp. 1–4.